Scaling of the vortex-liquid resistivity in optimally doped and oxygen-deficient $YBa_2Cu_3O_{7-\delta}$ single crystals

M. Andersson, A. Rydh, and Ö. Rapp
Department of Solid State Physics, KTH, SE-100 44 Stockholm, Sweden
(Received 19 December 2000; published 18 April 2001)

The consequences of a recently proposed model [A. Rydh, Ö. Rapp, and M. Andersson, Phys. Rev. Lett. **83**, 1850 (1999)] for the vortex-liquid resistivity close to a vortex liquid-to-glass transition are analyzed in detail. We find a detailed *quantitative* agreement between the model and resistivity measurements on disordered, optimally doped $YBa_2Cu_3O_{7-\delta}$ single crystals. For temperatures below the superconducting transition temperature, a scaling of all measured resistivity curves in magnetic field ($0<B\leqslant 12$ T) is obtained. Possible ways of slightly modifying the model in order to fully describe resistivity measurements on more anisotropic underdoped oxygen-deficient $YBa_2Cu_3O_{7-\delta}$ single crystals are suggested. The physical interpretation of the model and its connection to other models of the vortex-liquid resistivity are discussed. In particular, we find close connections to vortex glass models and to a generalized Coulomb gas model.

DOI: 10.1103/PhysRevB.63.184511 PACS number(s): 74.60.Ge, 74.25.Fy, 74.72.Bk

I. INTRODUCTION

In high temperature superconductors (HTS), the large broadening of the resistive transition in magnetic field is a direct consequence of thermal fluctuations in the vortex system. In fact, the parameters (high temperatures, large penetration depths, small coherence lengths and large electrical anisotropies) are all conspiring to increase the importance of thermal fluctuations in HTS.[1,2] Strong thermal fluctuations lead to the melting of a flux line lattice over a substantial part of the mixed state phase diagram in clean materials.[3] At temperatures below the melting temperature, T_m, the vortex system is in a (pinned) superconducting vortex-solid phase with nonzero critical current, while at $T>T_m$ it is in a dissipative vortex-liquid state. Signatures of a first order phase transition in clean samples are seen from measurements of the specific heat,[4] magnetization measurements,[5–7] and jumps in the resistivity.[8]

When disorder is introduced, the vortex-solid transforms into a glassy vortex state and the vortex solid-to-liquid transition becomes second order.[9–11] Depending on the type and strength of the disorder, different types of glassy solid states can be obtained, like, e.g., a vortex glass in the presence of point disorder[9] or a Bose glass in the presence of correlated disorder.[12] The glass phases will have different critical exponents depending on the type of disorder, but the overall behavior seen from an experimental point of view is rather similar. The linear resistivity disappears in all cases as a power law

$$\rho=\rho_0\left|\frac{T}{T_g}-1\right|^s \tag{1}$$

close to the glass transition temperature, T_g. s is here a combination of the universal critical exponents of the glass transition and is the only factor that is related to the kind of disorder giving the transition. From Eq. (1), ρ_0 is identified as a characteristic resistivity and should in some way be related to the normal state resistivity. This relation can either be direct through $\rho_0\propto\rho_n$ or indirect through the flux flow resistivity, ρ_{ff}, which is related to ρ_n through the Bardeen-Stephen equation, $\rho_{ff}=\rho_n B/B_{c2}(T)$, where B is the applied magnetic field and $B_{c2}(T)$ is the upper critical field.

From the formulation used in Eq. (1), there is no obvious connection between the glass resistivity itself and the basic superconducting parameters. However, in a real material, the superconducting condensation energy and thereby the pinning energy are changing with temperature and magnetic field. A detailed description of the glass transition in HTS should take this into account. We have recently proposed such a model and showed that it gives a consistent description of the vortex liquid resistivity at all magnetic fields in our study ($B\leqslant 12$ T).[13] Here, we further develop this model and relate it to other models usually used to describe the low resistivity part of the vortex liquid.

The outline of the paper is as follows. The model is first described in general and some useful relations are derived. Then, the experiments are described and an analysis of the resistivity in an optimally doped $YBa_2Cu_3O_{7-\delta}$ (YBCO) single crystal is made and shows that our model gives a detailed description of the experimental results. We show that the main ideas can be applied also to doped materials like oxygen-deficient YBCO single crystals. Finally, two possible physical interpretations of the model are discussed, one based on a vortex glass scenario and the other on a generalized Coulomb gas scaling.

II. MODEL

For the vortex glass model presented in Eq. (1), the linear resistivity close to T_g mainly depends on the distance to T_g and the relevant energy scales are therefore k_BT and k_BT_g. In a superconductor, however, energy scales as the condensation energy or the pinning energy are changing with *both* temperature and magnetic field. Therefore, as depicted in Fig. 1, one should consider the distance to the transition line $B_g(T)$ in the two-dimensional B-T diagram instead of the one-dimensional distance to T_g at constant B. Similar effects are well known from corrections to the temperature dependence of the superconducting condensation energy close to

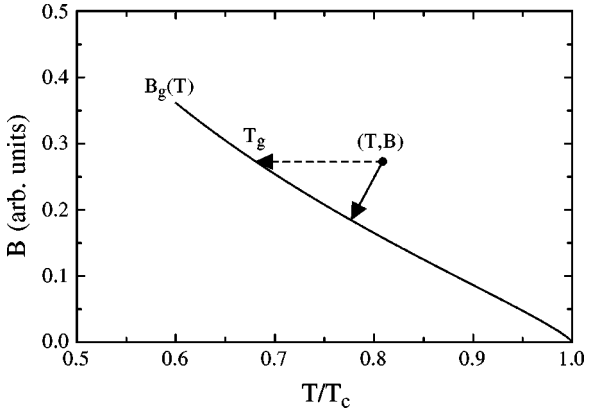

FIG. 1. Sketch of the principal physical idea behind our approach. The relevant energy scale, $U_0(B,T)$, at a specific point (T,B) in the vicinity of the vortex solid-to-liquid transition is determined by the distance to the *transition line*, $B_g(T)$, in a B-T diagram. This is in contrast to other approaches, where only the temperature distance to T_g is taken into acocunt. (The magnetic field has arbitrarily been scaled to the parameter B_0 discussed later on.)

B_{c2}. In a general description, we denote the relevant energy scale determining flux motion in the vortex liquid by $U_0(B,T)$ (at the moment, only the existence of such an energy scale is needed and we postpone the discussion concerning the interpretation of U_0). The linear resistivity caused by thermal fluctuations will be determined from the competition between $U_0(B,T)$ and the thermal energy, k_BT. In this picture, it is natural to assume that a specific resistivity level corresponds to a constant $U_0(B,T)/k_BT$, i.e., the resistivity scales as

$$\frac{\rho}{\rho_n}=F\left(\frac{U_0(B,T)}{k_BT}\right), \tag{2}$$

where F is a scaling function. Here, we have chosen to use the normal state resistivity ρ_n as the characteristic resistivity. This is based both on the empirical results presented below and on the fact that any characteristic energy should be related to ρ_n in some way. The vortex solid-to-liquid transition then occurs when the two relevant energy scales are equal, i.e., when

$$U_0(B,T_g)=k_BT_g. \tag{3}$$

Since disordered materials are discussed in the following, we denote the transition temperature by T_g as for a glass transition. The main arguments could possibly be valid also for the resistivity above a melting transition. The scaling function F is expected to have different functional dependences for different kinds of transitions. This means that one should not expect to find scaling for all magnetic fields if the nature of the transition changes with field, as for example is the case when passing the purported tricritical point in the B-T diagram of clean YBCO single crystals.[14] An interesting observation is that the proposed model directly suggests that a curve in the B-T diagram containing points of equal resistivity should follow the same behavior as the vortex solid-to-liquid line. This gives a natural explanation of the experimental fact that a determination of the solid-to-liquid transition line by different experimental methods give similar result although some methods, strictly speaking, only correspond to a constant (low) resistivity level.[15]

The main difficulty is to find the explicit field and temperature dependence of U_0. In the following, an approach to do this for a vortex glass transition is presented. It should be noted already here that differences from a conventional vortex glass model are rather subtle as far as the temperature dependence of the resistivity is concerned. In our picture, the characteristic energy $U_0(B,T)$ replaces the thermal energy at the glass transition line, k_BT_g, in the vortex glass expressions and thus gives a more detailed description of the resistivity at temperatures away from T_g. Since U_0 is expected to be a slowly varying function of temperature and the resistivity disappears rapidly close to T_g, it may seem hard to observe any differences between these two models from experiments. However, such differences can be detected by plotting the experimental data in a proper way, as will be shown below. The main advantage of the present model is that it gives a consistent and detailed description of the magnetic field dependence of the resistive transition.

A direct consequence of the arguments above and Eq. (1) is that the resistivity close to a vortex glass transition, should be written

$$\rho=\rho_n\left|\frac{k_BT}{U_0(B,T)}-1\right|^s, \tag{4}$$

where $U_0(B,T)$ has replaced k_BT_g as the relevant energy scale and we have put ρ_n as the prefactor in agreement with Eq. (2). To proceed, we note that a good scaling of the resistivity curves of disordered HTS was obtained empirically by writing the effective pinning energy[13]

$$U_0=k_BT_c\frac{1-T/T_c}{(B/B_0)^\beta}=U_B(1-T/T_c). \tag{5}$$

Here, B_0 and β are field and temperature independent constants, and hence the energy $U_B=k_BT_c/(B/B_0)^\beta$ is temperature independent. As will be shown below, this particularly simple form for U_0 is sufficient to give a detailed description of the vortex-liquid resistivity in an optimally doped, weakly disordered single crystal of YBCO for magnetic fields up to at least 12 T.

Although the exact interpretation of U_0 and the precise temperature and field dependencies are not completely clear, the form used in Eq. (5) is quite reasonable. One can, e.g., start from the basic energy scale determining the self-energy of a vortex line, $\epsilon_0\approx\Phi_0^2/4\pi\mu_0\lambda^2$, where Φ_0 is the flux quantum, μ_0 is the permeability of free space and $\lambda(T)$ is the temperature dependent penetration depth. In a Ginzburg-Landau approximation, $\lambda(T)=\lambda(0)(1-T/T_c)^{-0.5}$, which directly gives $\epsilon_0\propto(1-T/T_c)$. The power law in the field dependence is a characteristic feature for most analyses of the resistivity in a vortex liquid based on theories for thermally activated flux motion.[16–18] After having noted these

similarities with well established results, we will use Eq. (5) to derive some useful relations.

The first observation to be made is that Eqs. (3) and (5) immediately gives the temperature dependence of the vortex glass line,

$$B_g(T) = B_0\left(\frac{1-T/T_c}{T/T_c}\right)^{1/\beta}. \tag{6}$$

This relation has experimentally been shown to describe the vortex glass line very well for various HTS having different anisotropies.[19] Secondly, by instead considering $T_g(B)$ as obtained by inverting Eq. (6), the temperature independent energy U_B as defined in Eq. (5) can be written $U_B = k_B T_c T_g/(T_c - T_g)$, which leads to a reformulation of Eq. (5),

$$U_0 = k_B T_g \frac{T_c - T}{T_c - T_g}, \tag{7}$$

where the field dependence is implicit through the field dependence in $T_g(B)$. From Eqs. (4) and (7), we finally obtain the relation

$$\rho = \rho_n \left| \frac{T(T_c - T_g)}{T_g(T_c - T)} - 1 \right|^s, \tag{8}$$

which will turn out to be useful when analyzing the experimental data. Note that the field dependence of the resistivity only comes in through $T_g(B)$ in this relation.

From the similarities between Eqs. (1) and (4), it is clear that our description can be seen as a modification of the vortex glass theory. Let us therefore explore the consequences of these modifications and compare them with the ordinary theory. From Eq. (1), one directly obtains

$$\left(\frac{\partial \ln \rho}{\partial T}\right)^{-1} = \frac{T - T_g}{s}. \tag{9}$$

The usual way of extracting the vortex glass temperature is to calculate the inverse of the logarithmic derivative of Eq. (1) from experimental data and to extrapolate the plotted data to $(\partial \ln \rho/\partial T)^{-1} = 0$ in order to obtain T_g.[20] In our approach, we instead find

$$\left(\frac{\partial \ln \rho}{\partial T}\right)^{-1} = \frac{T - T_g}{s}\left(\frac{T_c - T}{T_c - T_g}\right) \tag{10}$$

by taking the logarithmic derivative of Eq. (8). The only difference between Eqs. (9) and (10) is a factor $(T_c - T)/(T_c - T_g)$, which is nearly one for temperatures sufficiently close to T_g. This establishes that Eq. (9) is still a good approximation in our case. Furthermore, by a series expansion of our expressions above T_g (see Appendix A), the resistivity can be written

$$\rho = \rho_n \left[\frac{1 + (B/B_0)^\beta}{T_c - T}\right]^s (T - T_g)^s. \tag{11}$$

This expression is similar to the one usually used for the resistivity close to a vortex glass transition, $\rho = \rho_0 (T - T_g)^s$. In fact, Eq. (11) can be considered as a more detailed description of the glass transition explicitly giving the field and temperature dependence of ρ_0. We see that the temperature dependence of ρ_0 is only slowly varying in the neighborhood of T_g. This once again indicates the similarities with the vortex glass picture.

There is also an interesting connection between our field dependence of U_0 and that found from analyzing the resistivity by models based on thermally assisted flux flow[21] (TAFF) or on plastic deformations[22] in the vortex system. In these models, the resistivity follows a temperature dependence, $\rho = \rho_1 \exp(-U^\star/k_B T)$, where the activation energy for flux motion, $U^\star$, is magnetic field dependent. Experimentally, $U^\star$ is obtained from the slope in an Arrhenius plot since we have

$$\frac{\partial \ln \rho}{\partial (1/T)} = -\frac{U^\star}{k_B}. \tag{12}$$

From Eq. (8), the same derivative can be calculated and we obtain

$$\frac{\partial \ln \rho}{\partial (1/T)} = -s \frac{U_B}{k_B} \frac{[1 + (\rho/\rho_n)^{1/s}]^2}{(\rho/\rho_n)^{1/s}}, \tag{13}$$

where the derivative has been rewritten in terms of the energy U_B as defined in Eq. (5) and the reduced resistivity, ρ/ρ_n. By comparing these two equations, it is seen that U_B and $U^\star$ will have the same field dependence provided that the slope in the Arrhenius plots are taken at a constant ρ/ρ_n, which is almost always the case in experimental studies. As discussed below, there is even a quantitative agreement between these two equations when analyzing the experimental data.

The equations above were all derived for a particular simple form of the characteristic energy $U_0(B,T)$ in Eq. (5). A more general discussion is given in Appendix B.

III. EXPERIMENT

Single crystals of YBCO were grown by a self-flux method in yttria stabilized zirconia crucibles as previously described.[23] Twinned crystals of varying oxygen content were obtained by annealing for 3–7 days at various temperatures ranging from 450°C to 700°C. The oxygen-deficient samples were annealed in air, while the optimally doped one was annealed in flowing oxygen. A summary of the annealing conditions and some important parameters are shown in Table I.

Electrical contacts were prepared by applying strips of silver paint, followed by heat treatment under the same conditions as during annealing, giving contact resistances below 1.5 Ω. Typical dimensions of the samples were $0.5 \times 0.2 \times 0.03$ mm^3. Measurements of the in-plane resistance for magnetic fields $0 \leqslant B \leqslant 12$ T applied along the crystallographic *c*-axis were made in a flowing gas cryostat. The samples were placed in a vacuum space inside the variable temperature insert of the cryostat to protect them from temperature variations in the flowing gas. A current of $I = 0.3$ mA was used and a voltage resolution down to 0.3 nV

TABLE I. Annealing conditions, transition temperature T_c, transition width ΔT_c, and anisotropy parameter γ of the studied $YBa_2Cu_3O_{7-\delta}$ single crystals.

Sample	Annealing	T_c (K)	ΔT_c (K)	γ
1	O_2, 450 °C	91.3	0.15	8.7
2	air, 500 °C	86.2	1.0	13
3	air, 525 °C	73.2	2.5	19
4	air, 700 °C	51.8	2.0	35

was achieved with the use of a dc picovoltmeter as preamplifier. The samples were cooled in field through the superconducting transitions and data were recorded during increasing temperatures.

IV. OPTIMALLY DOPED SINGLE CRYSTALS

We start by discussing the vortex-liquid resistivity in optimally doped single crystals of YBCO with a small amount of disorder. The defects in the crystal described here consisted of twin boundaries, point defects from adatoms in the starting materials and oxygen disorder (increasingly important for the oxygen-deficient samples). The resistivity showed a glassy behavior at all magnetic fields studied, which is believed to come mainly from point disorder.[13] $\rho(B,T)$ of the optimally doped sample (sample 1) is shown in the Arrhenius plot in Fig. 2. The zero field transition has a width of 0.15 K and the resistivity has a low value of about 70 $\mu\Omega$ cm just above T_c, showing the good sample quality. Furthermore, the normal state resistivity extrapolates to zero as shown in the inset of Fig. 2. This extrapolated line has been taken as the normal state resistivity, ρ_n, in all the analyses presented below.

We start our analysis by considering the vortex glass temperature, which is usually obtained from Eq. (9). In our model, however, the situation becomes more complicated due to the correction factor $A(T)=(T_c-T)/(T_c-T_g)$ in Eq. (10), which gives an implicit equation for T_g. However, the correction factor is roughly one close to T_g and it is possible

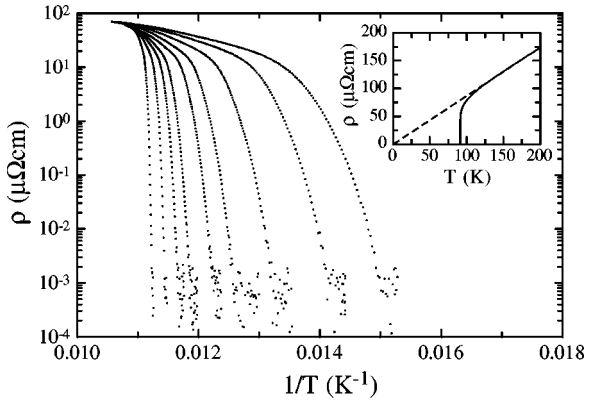

FIG. 2. Arrhenius plot of the resistivity for optimally doped YBCO single crystal for (from left to right) $B=0.5$, 1, 1.5, 2, 3, 4, 6, 9, and 12 T. Inset: Extrapolation of the normal state resistivity to zero.

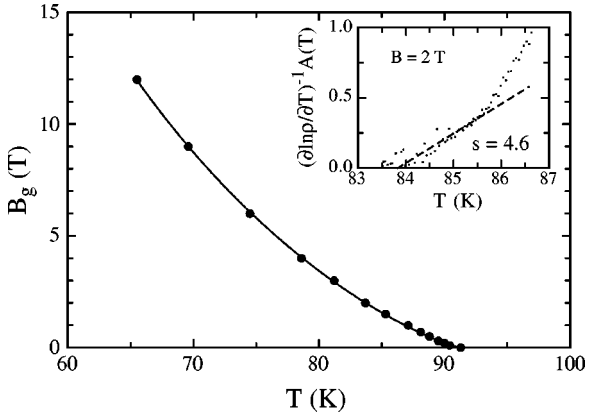

FIG. 3. Field dependence of the vortex glass line. Solid points were determined as shown in the inset. The solid curve is a fit to Eq. (6) with $B_0=36.9$ T and $\beta=0.83$. Inset: Determination of the glass transition temperature from Eq. (10). Here $A(T)=(T_c-T_g)/(T_c-T)$ is the correction factor to the result for an ordinary vortex glass in Eq. (9).

to find a good value of T_g from Eq. (9) in a first approximation. In a second approach, one can use this T_g for a more detailed analysis as shown in the inset of Fig. 3. As predicted by Eq. (10), a linear relation is found close to T_g between temperature and $A(T)(\partial \ln\rho/\partial T)^{-1}$. The differences in T_g between these two approaches lies within the experimental errors of the extrapolations and can be neglected for most practical purposes. One may also expect a difference in the linearity of the data close to T_g when comparing Eq. (9) and Eq. (10). We have not been able to distinguish any clear such difference from our analyses due to the noise level in this regime.

The main part of Fig. 3, shows the field dependence of the vortex glass transition. As shown by the solid curve, a good fit to Eq. (6) is obtained. The fitting parameters are $B_0=36.9$ and $\beta=0.83$. For this sample, we also note that a reasonable fit can be obtained by the ordinary vortex glass expression, $B_g \propto (1-T/T_c)^n$, with $n=1.4$. Such an expression will, however, not give the consistent description discussed below.

As previously discussed, it is not possible to find a definite proof for our approach from the differences between Eqs. (9) and (10). A much more sensitive test is provided by Eq. (4). By solving for U_0, one obtains

$$U_0(B,T)=k_BT\left[1+\left(\frac{\rho}{\rho_n}\right)^{1/s}\right]^{-1}. \tag{14}$$

$U_0(B,T)$ can therefore be calculated directly from experimental data provided that one knows the exponent s and $\rho_n(T)$. s is easily obtained as the inverse slope in Eq. (10) and the normal state resistivity is determined by the linear extrapolation shown in the inset of Fig. 2. The result of this analysis is shown in Fig. 4, where U_0 is shown as a function of temperature at different magnetic fields. A striking feature is the linear behavior of $U_0(T)$ at the lowest temperatures (i.e., closest to T_g). When extrapolating this linear behavior at different fields, one realizes that the lines all merge in

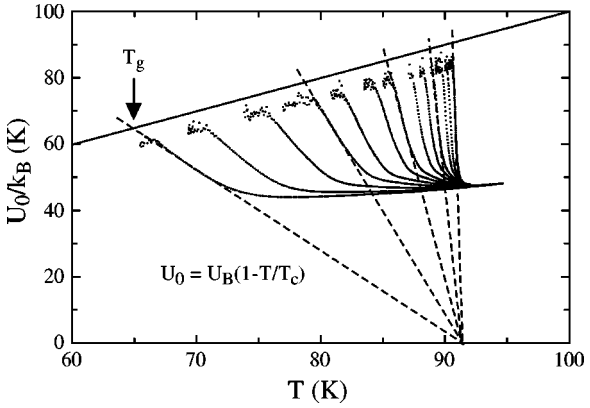

FIG. 4. The energy U_0 as obtained from Eq. (14) for (from left to right) $B=12$, 9, 6, 4, 3, 2, 1.5, 1, 0.7, 0.5, 0.3, 0.2, and 0.1 T. As clearly shown by the dashed lines, the low resistivity parts of the curves are well described by Eq. (5) with a field dependent U_B. The glass transition temperature is obtained when U_0 crosses the solid line $U_0=k_BT$.

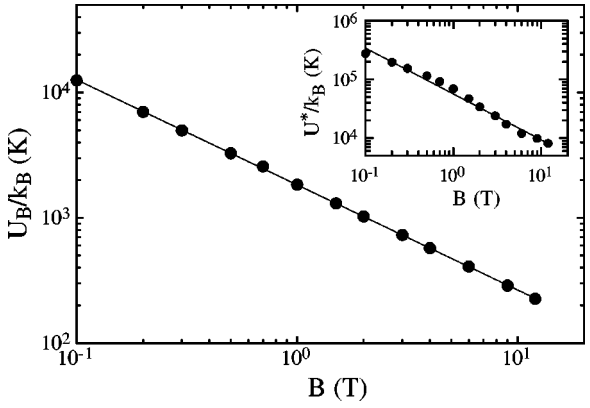

FIG. 5. Magnetic field dependence of U_B as obtained from Eq. (5) and the slopes in Fig. 4. The solid line is a fit to the data giving the relation $U_B/k_B=1831B^{-0.84}$. Inset: Activation energies obtained by analyzing the resistivity within a TAFF model. The solid line is a fit to the points with the equation, $U^\star/k_B=(5.7\times10^4)B^{-0.78}$ with B in T.

the point $T=T_c$ and $U_0=0$. *Therefore, Fig. 4 immediately shows that one can write* $U_0=U_B(1-T/T_c)$ *as stated in Eq. (5).* Furthermore, T_g can be directly obtained from Fig. 4 by considering the crossing points of the lines $U_0(T,B)$ and the line $U_0=k_BT$, which is the criterion we used for finding T_g in Eq. (3). We therefore conclude that Fig. 4 gives strong evidence for the proposed model.

Another important point is that the temperature dependence of U_0 illustrated by Fig. 4 directly shows that the ordinary vortex glass expression is insufficient for describing the data. For an ordinary vortex glass model, one expects a horizontal line since Eq. (1) implies a constant $U_0(B)=k_BT_g(B)$ at all temperatures close to T_g. This is obviously not the case in Fig. 4.

A potentially weak point in our argumentation is the way we have chosen the parameters s and ρ_n. We have therefore slightly changed the parameters to investigate the sensitivity of the analysis in Fig. 4. For changes in s within the uncertainty limits given by the extrapolations used in Fig. 3, there are only small changes in Fig. 4. In brief, the lines become somewhat curved and the crossing point shifts slightly from the point $T=T_c$ and $U_0=0$. The analysis is also rather robust to changes in ρ_n. However, if one considers large changes in the parameter ρ_n by more than one order of magnitude (requiring another physical meaning of the prefactor), the slopes in Fig. 4 change and there is no crossing point. Even when attempting such large changes, it is not possible to obtain constant U_0 at all magnetic fields, which again shows that our data are incompatible with the ordinary vortex glass theory.

We now discuss the magnetic field dependence of U_0. From Eq. (5), it is clear that the field dependence only comes in through the term U_B. U_B can in principle be found directly from the slopes in Fig. 4. A more convenient way is, however, to calculate $U_B=U_0/(1-T/T_c)$ from the experimental data and to plot $U_B(T)$. This gives a temperature independent and constant value of U_B (within $\pm2\%$) at each magnetic field as briefly reported previously.[24] The magnetic field dependence of U_B is shown in Fig. 5, where a power law dependence is found over an extended magnetic field region from 0.1 to 12 T. A fit to the data gives $U_B/k_B=1831B^{-0.84}$ with B in T. First, we note that we obtain the same exponent, β, for the magnetic field dependence in this analysis as in the analysis of the glass transition line (Fig. 3). Secondly, the prefactor in this fit is equal to $k_BT_cB_0^\beta$ according to Eq. (5). From this relation we calculate $B_0=37.1$ T in excellent agreement with the fit to $B_g(T)$ with $B_0=36.9$ T in Fig. 3. This shows the *quantitative* consistency of our analyses and the relationship between the glass transition line at $T=T_g$ and the characteristic energy U_0 at temperatures $T>T_g$, which is inherent in our model.

One can also find a qualitative agreement between our model and previous models of the vortex liquid resistivity based on a thermally activated behavior, despite the fact that the physics behind these models are different. As seen in the Arrhenius plots in Fig. 2, the resistivity in our sample can to a reasonably good approximation be described by a thermally activated behavior, $\rho=\rho_1\exp(-U^\star/k_BT)$. The field dependence of the activation energies determined in this way, using resistivity levels between 5×10^{-3} and 5×10^{-1} $\mu\Omega$ cm, are shown in the inset of Fig. 5. Although the data is somewhat scattered, a fit to a power law behavior gives $U^\star/k_B=(5.7\times10^4)B^{-0.78}$ with B in T, i.e., roughly the same field dependence as for U_B, where the exponent $\beta=0.83$ was obtained. Furthermore, the prefactor in the field dependence of $U^\star$ can be directly compared with the prefactor in the field dependence of U_B in Eq. (13). From this comparison, we find that the prefactors are equal when $\rho/\rho_n\approx1\times10^{-3}$, which corresponds to a resistivity level of about $(5-8)\times10^{-2}$ $\mu\Omega$ cm in good agreement with the resistivity region used for determining $U^\star$. Our model thus gives a good quantitative description of both $\rho(B,T)$ and its logarithmic temperature derivative close to T_g.

Equation (8) also predicts a scaling behavior between the normalized resistivity, ρ/ρ_n, and the scaled temperature $T(T_c-T_g)/T_g(T_c-T)-1$, with $T_g=T_g(B)$. Such a scaling

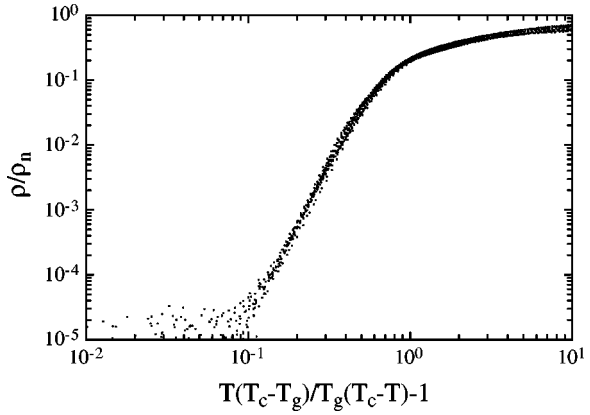

FIG. 6. Normalized resistivity versus scaled temperature according and 12 T. The slope of the curve gives the critical exponent, $s=4.6\pm0.3$.

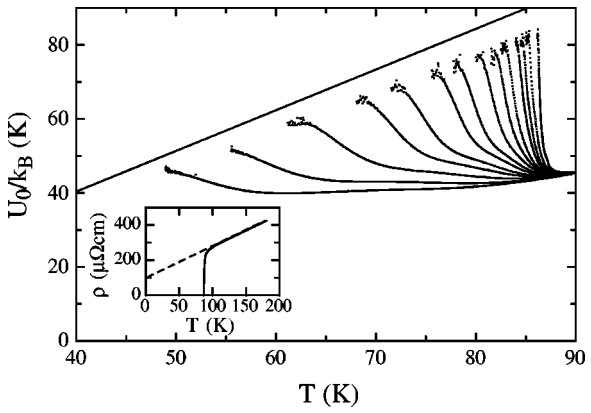

FIG. 7. Characteristic features of our oxygen-deficient crystals shown here for sample 2 ($T_c=86.2$ K). As clearly seen, the simple description of U_0 used for the optimally doped crystal in Fig. 4 cannot be used. Inset: Extrapolated normal state resistivity versus temperature for this sample.

is shown in Fig. 6, where the resistive transitions at 13 fields between 0.1 and 12 T have been scaled onto one curve (most of the resistivity curves are shown in Fig. 2). From the slope in Fig. 6, we find the critical exponent $s=4.6$ in agreement with previous analyses using Eq. (10) and data from Fig. 3. An interesting point is that the scaling also works for temperatures close to T_c, although the derivation above was only made for temperatures close to T_g. This clearly indicates that the general arguments we have used are of fundamental nature for understanding the full behavior of the vortex liquid. The analysis presented above has been made on data taken as a function of temperature at constant magnetic field. However, the scaling works equally well on data taken as a function of magnetic field at constant temperature.[25]

V. UNDERDOPED SINGLE CRYSTALS

We now apply this model to oxygen-deficient crystals in the underdoped regime of HTS. With decreasing total oxygen content in the crystals, oxygen is successively removed from the CuO chains lying in between the superconducting CuO_2 planes. This results in a decreased conductivity in the chains and thereby a decreased coupling between the CuO_2 planes which is equivalent to a higher electrical anisotropy as observed in many studies on YBCO.[19,26,27] Since the oxygen content can be easily controlled by annealing conditions, oxygen-deficient single crystals of YBCO is a suitable test system for vortex dynamics in HTS.

The general features of U_0 as obtained from Eq. (14) are shown in Fig. 7 for one of the oxygen-deficient samples. First, we note that the ordinary vortex glass equation will not be applicable for these samples either since we do not obtain a constant value of $U_0(T)$ as required. This conclusion remains unaltered even if the parameters s and ρ_n used for the calculation of U_0 are chosen far outside of their expected ranges. Secondly, the simple expression for U_0 used to describe the optimally doped sample in Fig. 4 is clearly not sufficient here. Below, we give two possible ways to generalize our picture in order to describe these data.

The first approach is based on a generalized temperature dependence of U_0. This is a natural extension, since U_0 in our case is expected to be related to the average pinning energy and thus to the superconducting condensation energy.[13] In this picture, one can consider many different choices for $U_0(T)$. As a first approximation, we have considered a power law behavior, $U_0=U_B(1-T/T_c)^m$, where the exponent m is a fitting parameter common for all resistivity curves and the magnetic field dependence is contained in the prefactor U_B, which is taken as a constant at each magnetic field. The low resistivity parts of the curves are fitted to a power law in the scaling variable k_BT/U_0-1, and the results give a fairly good scaling as shown in Fig. 8(a). This analysis is rather to be seen as qualitative evidence that the present theory can describe also these data since the explicit temperature dependence of U_0 is unknown and there are difficulties in determining a correct T_c to be used in the analysis. Here, we have defined T_c at every resistivity level as the temperature at which the zero field curve has the same resistivity, in order to compensate for the width of the superconducting transition. This gives a better scaling than considering a constant temperature like the 50% level of the normal state resistivity or the zero resistivity point. However, at the lowest magnetic fields, the scaling becomes sensitive to the choice of T_c. This can to some extent explain the small deviations observed in the upper part of the curve.

The second approach is to naively use Eq. (8), although such a scaling may not be expected from the plots of U_0 in Fig. 7. However, as seen in Fig. 8(b), this apparently gives a better scaling of the data over the whole temperature range from T_g to T_c. We also note that the curve is not perfectly linear in the low resistivity regime. Therefore, a power law relation between ρ/ρ_n and the scaling variable $T(T_c-T_g)/T_g(T_c-T)-1$ is strictly speaking not correct as was implicitly assumed when calculating U_0. This may then give a plausible explanation for the observed deviations from a $U_0=U_B(1-T/T_c)$ behavior in Fig. 7.

As seen in Fig. 9, this approach also gives a reasonable scaling for sample 3 and 4. In sample 4, there are larger deviations close to T_c in the scaling, which occurs at both the lowest ($B<0.5$ T) and at the highest ($B>6$ T) fields. First,

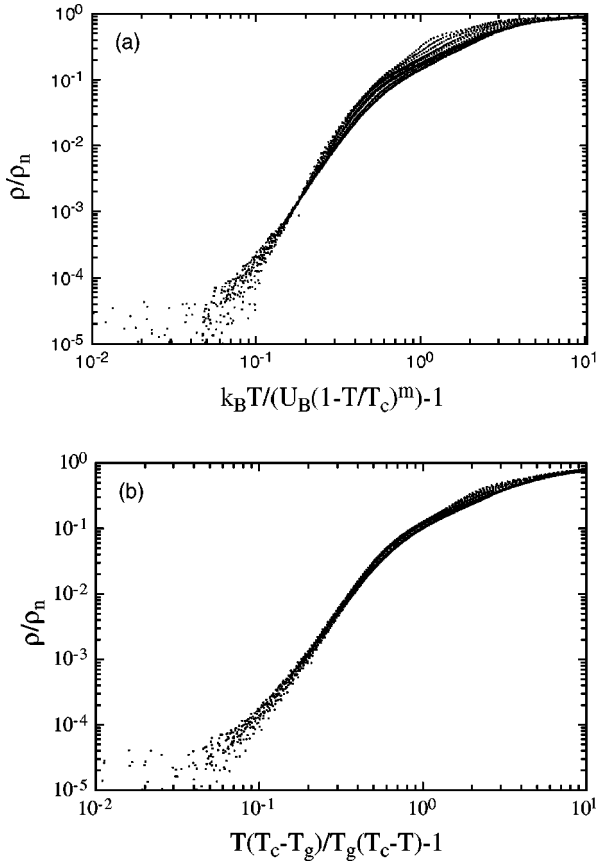

FIG. 8. Scaling attempts of the resistivity curves for sample 2 using (a) $U_0 = U_B(1 - T/T_c)^m$ with $m = 0.75$ and (b) the scaling form in Eq. (8). The scaling is shown for magnetic fields $0.5 \leqslant B \leqslant 12$ T.

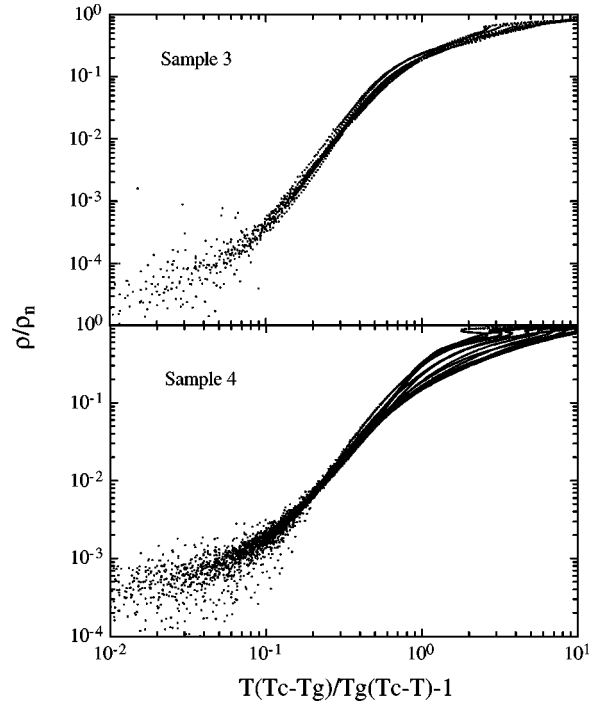

FIG. 9. Scaling according to Eq. (8) for samples 3 and 4.

there is a broadening of the fluctuation region above T_c in this sample indicating that there may be small regions in the sample with a somewhat higher T_c. This affects the analysis in the upper part of the transition by giving an uncertainty in the determination of T_c (taken as the temperature at which the zero field curve has the same resistivity). Such an effect will be particularly important at the lowest fields. Secondly, we have not considered any magnetic field dependence of T_c in our analysis. This effect will be most important at high fields in samples with low B_{c2} and for temperatures close to T_c, i.e., it may explain the deviations we observe at high fields.

Although we cannot unambiguously distinguish between different approaches for the underdoped samples, the reasonable scaling of the resistive curves obtained in Fig. 8 clearly suggests that the underlying ideas are still valid. This gives support for a general description of the vortex-liquid regime in HTS materials based on these results.

VI. DISCUSSION

Experimentally, our approach gives a fully consistent description of the vortex-liquid resistivity at all fields studied in an optimally doped YBCO single crystal. It also gives a good qualitative (or even semiquantitative) description of the field dependent resistivity in underdoped samples. This strongly suggests a direct connection between these results and the fundamental properties of the vortex liquid and thus of phase fluctuations in the superconducting condensate of HTS. However, when it comes to an understanding of the fundamental processes, the picture is still ambiguous. Two possible scenarios are discussed below based on interpretations of the scaling obtained for the underdoped samples.

The first scenario starts with the observation that the resistivity disappears as a power law (see Fig. 6). As shown by Eq. (11), this scaling implies that in a first approximation, the resistivity close to T_g disappears as a power law in $T - T_g$ as predicted for a second order phase transition like the vortex glass or Bose glass transitions.[9,12] It is natural to assume that the characteristic energy $U_0(B,T)$ is related to the effective average pinning energy in the system. The vortex solid-to-liquid transition occurs when $U_0(B,T_g) = k_B T_g$ as discussed above. Here, it is important to make a clear distinction between the average pinning energy, U_0, and the activation energy for flux motion, $U^\star$. $U^\star$ diverges at T_g due to the diverging glass correlation length in the vortex liquid, while U_0 only changes slowly with B and T when passing T_g. This can also be seen directly by comparing Eqs. (12) and (13). While $U_0 = U_B(1 - T/T_c)$ remains finite for $T = T_g$, $U^\star \propto \partial \ln \rho / \partial(1/T) \propto \rho^{-1}$ diverges, since ρ in Eq. (13) becomes zero at T_g. This distinction is similar to the one made in collective pinning theory between the underlying average energy scale and the relevant energy scale for flux motion, where the latter is obtained by a summation of the average energy scale taken over the coherently jumping volume.[2] The difference in our case is that the changes in the coherence volume is driven by the diverging glass correlation length (and time) due to the proximity to T_g.

This description works very well for the optimally doped sample. For underdoped samples, a good scaling of the low resistance part of the transition is also obtained by allowing for a generalized temperature dependence of U_0. In contrast to the optimally doped sample, this approach can seemingly not be extended to the region close to T_c. Starting from a description based on a glass transition, one would a priori not expect the scaling to work close to T_c. It is then surprising to find that the scaling works so well for the optimally doped sample. As suggested above, the transition is connected to the energy scale U_0, which is connected to the superconducting condensation energy and therefore goes to zero at T_c. If this follows a specific relation, one would in our model also expect the resistivity to scale close to T_c, since it is the same energy scale that determines the resistivity both close to T_g and close to T_c.

The second scenario is based on the observation that the vortex liquid resistivity scales as a function of $T(T_c - T_g)/T_g(T_c - T) - 1$ as shown in Figs. 6 and 8. For the optimally doped sample, the resistivity disappears with a power law behavior as seen in Fig. 6. However, for the underdoped sample in Fig. 8 there is no clear power law behavior at low resistivities. One may consider several possible explanations such as the signature of a cutoff in the glassy behavior for example caused by screening[28] or a crossover between two glassy behaviors with different critical exponents. This would then explain the observation in Fig. 7 that the apparent U_0 calculated from the assumption of a glass transition deviates from the behavior observed for the optimally doped sample.

Interestingly, the scaling factor used for the temperature in Figs. 6 and 8 is similar to the one predicted for the Coulomb gas scaling used to describe a zero-field two-dimensional Kosterlitz-Thouless transition.[29,30] In that case, T_g is replaced with the Kosterlitz-Thouless temperature, T_{KT}, and $X = T(T_{c0} - T_{\mathrm{KT}})/T_{\mathrm{KT}}(T_{c0} - T)$ is the scaling parameter, where T_{c0} is the superconducting transition temperature. In HTS, such a scaling has previously been used for describing the zero-field resistivity in $YBa_2Cu_3O_{7-\delta}/PrBa_2Cu_3O_{7-\delta}$ multilayers.[31] Recently, a modified scaling law has also been shown to describe the field dependent resistivity (up to 5 T) in $Bi_{2+y}Sr_{2-x-y}La_xCuO_{6+\delta}$ (BSLCO) thin films.[32] These authors found a clear relation between the scaling relations and the field dependence of the thermally activated resistivity for vortex motion similar to our results.[24] In their description, the resistive tails were assumed to be described by the Halperin-Nelson relation[33] $R(T,B) = R_n \exp[-A/(X-1)^{0.5}]$, where A is a constant. This implies a scaling relation, $\ln[R/R_n] = -A/(X-1)^{0.5}$, which has been shown to give a good description of all the data in the vortex liquid regime of an optimally doped BSLCO thin film.[32] In our case, the resistivity tail of the optimally doped sample is instead described by a power law as expected for a second order phase transition.

A plausible explanation for these different behaviors comes from the large differences in electrical anisotropy between the systems. In optimally doped YBCO, the anisotropy $\gamma \approx 8$, results in an almost three-dimensional vortex system. The anisotropy in BSLCO is very large, of the order of $\gamma \approx 100-200$, thus implying a quasi-two-dimensional vortex system, with possibly independent pancake vortices in each superconducting layer (due to weak coupling along the c axis). This will certainly affect the scaling of the resistivity just above T_g. The small deviations we observe in the underdoped samples as compared to the optimally doped one, may in fact be a consequence of change in behavior when going from an almost three-dimensional vortex system towards a quasi-two-dimensional one with increased anisotropy.

In summary, we have shown that the resistive transition curves in magnetic fields of optimally doped and underdoped disordered YBCO single crystals can be scaled and described in a consistent way. In the case of optimally doped crystals, we find a detailed quantitative description of the vortex liquid resistivity and its derivatives close to T_g. In addition, the scaling analysis suggested from this model is shown to be applicable for the whole vortex liquid regime. We have also discussed possible extensions of our model to allow for a detailed description of the vortex liquid in underdoped YBCO single crystals. Finally, two possible physical interpretations of our model based on a vortex glass and a generalized Coulomb gas scenario have been discussed.

ACKNOWLEDGMENTS

Financial support from the Swedish Natural Science Research Council, the Swedish Research Council for Engineering Sciences, and the Swedish Superconductivity Consortium is gratefully acknowledged.

APPENDIX A: COMPARISON WITH VORTEX GLASS THEORY

A first order series expansion in U_0 around T_g gives

$$k_B T - U_0 \approx \left[k_B - \left(\frac{\partial U_0}{\partial T} \right)_{T_g} \right] (T - T_g) = k_B T_c \frac{T - T_g}{T_c - T_g}, \tag{A1}$$

where we have used Eq. (7) in the last equality to calculate $\partial U_0/\partial T$ at the glass transition temperature. Furthermore, from the glass transition line, Eq. (6),

$$T_g(B) = T_c \left[1 + \left(\frac{B}{B_0} \right)^{\beta} \right]^{-1}. \tag{A2}$$

Putting this together with the description of the resistivity in Eq. (4), we finally obtain

$$\rho = \rho_n \left[\frac{1 + (B/B_0)^{\beta}}{T_c - T} \right]^s (T - T_g)^s. \tag{A3}$$

APPENDIX B: TEMPERATURE DEPENDENCE OF U_0

Our model can easily be generalized to the situation where $U_0(B,T)$ has a different temperature dependence. Let us consider the situation where the field and temperature dependencies of U_0 can be separated from each other, i.e.,

$$U_0 = U_B f(T), \tag{B1}$$

where U_B contains the magnetic field dependence and $f(T)$ is a general function of temperature. U_0 is here considered to be the effective pinning energy in the system and is therefore related to the condensation energy in the superconducting state. As before, we expect the vortex solid-to-liquid transition to occur when $U_0(B,T_g) = k_B T_g$, which gives $U_B = k_B T_g / f(T_g)$. Thus, U_0 can be written

$$U_0 = k_B T_g \frac{f(T)}{f(T_g)} \tag{B2}$$

and Eq. (4) gives

$$\rho = \rho_n \left| \frac{T f(T_g)}{T_g f(T)} - 1 \right|^s . \tag{B3}$$

Taking the logarithmic temperature derivative of Eq. (B3) and inverting, we obtain the extrapolation formula used to determine the transition temperature

$$\left(\frac{\partial \ln \rho}{\partial T} \right)^{-1} = \frac{T - T_g}{s} \left[\frac{1 - \frac{T_g}{f(T_g)} \left(\frac{\partial f}{\partial T} \right)_{T_g}}{1 - \frac{T}{f(T)} \left(\frac{\partial f}{\partial T} \right)_{T}} \right], \tag{B4}$$

where the indices on the derivatives mark the temperature at which they should be evaluated. To derive Eq. (B4), we have also used a first order series expansion of $f(T)$ around $T = T_g$.

[1] C. J. Lobb, Phys. Rev. B **36**, 3930 (1987).
[2] G. Blatter, M. V. Feigel'man, V. B. Geshkenbein, A. I. Larkin, and V. M. Vinokur, Rev. Mod. Phys. **66**, 1125 (1994).
[3] A. Houghton, R. A. Pelcovits, and A. Sudbø, Phys. Rev. B **40**, 6763 (1989).
[4] A. Schilling, R. A. Fisher, N. E. Phillips, U. Welp, D. Dasgupta, W. K. Kwok, and G. W. Crabtree, Nature (London) **382**, 791 (1996).
[5] R. Liang, D. A. Bonn, and W. N. Hardy, Phys. Rev. Lett. **76**, 835 (1996).
[6] T. Nishizaki, Y. Onodera, N. Kobayashi, H. Asaoka, and H. Takei, Phys. Rev. B **53**, 82 (1996).
[7] U. Welp, J. A. Fendrich, W. K. Kwok, G. W. Crabtree, and B. W. Veal, Phys. Rev. Lett. **76**, 4809 (1996).
[8] H. Safar, P. L. Gammel, D. A. Huse, D. J. Bishop, J. P. Rice, and D. M. Ginsberg, Phys. Rev. Lett. **69**, 824 (1992).
[9] D. S. Fisher, M. P. A. Fisher, and D. A. Huse, Phys. Rev. B **43**, 130 (1991).
[10] R. H. Koch, V. Foglietti, W. J. Gallagher, G. Koren, A. Gupta, and M. P. A. Fisher, Phys. Rev. Lett. **63**, 1511 (1989).
[11] M. Charalambous, R. H. Koch, T. Masselink, T. Doany, C. Feild, and F. Holtzberg, Phys. Rev. Lett. **75**, 2578 (1995).
[12] D. R. Nelson and V. M. Vinokur, Phys. Rev. B **48**, 13 060 (1993).
[13] A. Rydh, Ö. Rapp, and M. Andersson, Phys. Rev. Lett. **83**, 1850 (1999).
[14] G. W. Crabtree, W. K. Kwok, L. M. Paulius, A. M. Petrean, R. J. Olsson, G. Karapetrov, V. Tobos, and W. G. Moulton, Physica C **332**, 71 (2000).
[15] See, e.g., E. H. Brandt, Rep. Prog. Phys. **58**, 1465 (1995).
[16] Y. Yeshurun and A. P. Malozemoff, Phys. Rev. Lett. **60**, 2202 (1988).
[17] T. T. M. Palstra, B. Batlogg, R. B. van Dover, L. F. Schneemeyer, and J. V. Waszczak, Phys. Rev. B **41**, 6621 (1990).
[18] M. Andersson, Yu. Eltsev, B. Lundqvist, A. Rydh, and Ö. Rapp, Physica C **332**, 86 (2000).
[19] B. Lundqvist, A. Rydh, Yu. Eltsev, Ö. Rapp, and M. Andersson, Phys. Rev. B **57**, R14064 (1998).
[20] H. Safar, P. L. Gammel, D. J. Bishop, D. B. Mitzi, and A. Kapitulnik, Phys. Rev. Lett. **68**, 2672 (1992).
[21] P. H. Kes, J. Aarts, J. van den Berg, C. J. van der Beek, and J. A. Mydosh, Supercond. Sci. Technol. **1**, 242 (1989).
[22] V. M. Vinokur, M. V. Feigel'man, V. B. Geshkenbein, and A. I. Larkin, Phys. Rev. Lett. **65**, 259 (1990).
[23] Yu. Eltsev, W. Holm, and Ö. Rapp, Phys. Rev. B **49**, 12 333 (1994).
[24] M. Andersson, A. Rydh, and Ö. Rapp, Physica C **341-348**, 1239 (2000).
[25] A. Rydh, Ö. Rapp, and M. Andersson, Physica B **284-288**, 707 (2000).
[26] T. R. Chien, W. R. Datars, B. W. Veal, A. P. Paulikas, P. Kostic, Chun Gu, and Y. Jiang, Physica C **229**, 273 (1994).
[27] J. Deak, Lifang Hou, P. Metcalf, and M. McElfresh, Phys. Rev. B **51**, 705 (1995).
[28] H. S. Bokil and A. P. Young, Phys. Rev. Lett. **74**, 3021 (1995).
[29] J. M. Kosterlitz and D. J. Thouless, J. Phys. C **6**, 1181 (1973).
[30] P. Minnhagen, Rev. Mod. Phys. **59**, 1001 (1987).
[31] P. Minnhagen and P. Olsson, Phys. Rev. B **45**, 5722 (1992).
[32] Y. Z. Zhang, R. Deltour, and Z. X. Zhao, Phys. Rev. Lett. **85**, 3492 (2000).
[33] B. I. Halperin and D. R. Nelson, J. Low Temp. Phys. **36**, 599 (1979).